Supporting Information

Supporting Information Materials and Methods

In-gel digestion

Gel pieces were sliced into ~1 mm^3 cubes and de-stained with 50 mM ammonium bicarbonate in a 50% ACN aqueous solution at 37˚C for 45 min. Subsequently, the gel pieces were dehydrated in 70% ACN, then 100% ACN, reduced with 10 mM DTT, and alkylated with 50 mM iodoacetamide. The gel pieces were once again washed and dehydrated. After the gels were fully dried, they were rehydrated with 25 ng/μL of sequencing-grade trypsin in freshly prepared reaction buffer (50 mM ammonium bicarbonate, 0.1 mM $CaCl_2$, pH 8.0). Any remaining solution was discarded from the gels, and 50 μL of additional reaction buffer was added. After overnight incubation at 37°C, 50 μL of 10% formic acid/10% ACN solution was added, and the digested peptides were extracted by ultrasonication. Then, the peptides were extracted using 100 μl of a 0.1% trifluoroacetic acid (TFA)/50% ACN solution, followed by a 0.1% TFA/70% ACN solution, and finally a 0.1% TFA/100% ACN solution. The collected peptides were dried in a SpeedVac vacuum evaporator and reconstituted in 10 μL of 0.1% formic acid in distilled water. The samples were centrifuged prior to LC-MS/MS injection.

Solvent gradients and parameters for the LC-MS/MS analysis

The peptides were eluted using the mobile phase gradient of solvent A (0.1% formic acid in water) and B (0.1% formic acid in ACN) with a flow rate of 200 nL/min. The gradient started with 2% solvent B and increased to 50% by 100 min, then increased to 100% by 105 min. After 5 min of maintaining 100% solvent B (washing), the column was equilibrated with 98% solvent A and 2% solvent B for another 10 min. The eluted peptides were ionized by nanospray with a voltage of 1.4 kV and submitted to the mass spectrometer. Peptide ions were first analyzed with a full-MS scan in a range of 300-2000 m/z, and the top 7 most intense ions from the full-MS scan were data-dependently selected for CID tandem MS analysis (normalized collision energy of 35 for 30 msec). The following dynamic exclusion parameters of the data-dependent scan were used: repeat count = 2, repeat duration = 30 sec, list size = 300, exclusion duration = 180 sec, low mass width = 0.8, and high mass width = 2.2.

Protein identification through database searching

In detail, SEQUEST was searched with a fragment ion mass tolerance of 1.00 Da and a parent ion tolerance of 1.00 Da. Iodoacetamide derivatives of cysteine and methionine oxidation were specified as a fixed modification and a variable modification, respectively. Peptide identifications were accepted if they exceeded the following thresholds: DeltaCn scores greater than 0.10 and XCorr scores greater than 1.8, 2.5, 3.5 and 3.5 for singly, doubly, triply, and quadruply charged peptides. Protein identifications were accepted if they contained at least 2 identified peptides, and proteins that contained similar peptides that could not be differentiated based on MS/MS analysis alone were grouped to satisfy the principles of parsimony.

Table S1. List of the down-regulated secretory proteins (70 proteins).

Gene symbol	Accession #	MW	Mean ± SD of Control	Mean ± SD of GKB treated	*p* value[a]	Rsc[a]
ADAM9	IPI00440932	91	0.8 ± 0.5	0.0 ± 0.0	0.039	-∞
AGRN	IPI00374563	215	0.9 ± 0.2	0.0 ± 0.0	0.003	-∞
ATRN	IPI00162735	141	1.0 ± 0.4	0.0 ± 0.0	0.010	-∞
B4GALT1	IPI00215767	44	0.7 ± 0.4	0.0 ± 0.0	0.038	-∞
BMP1	IPI00009054	111	2.3 ± 0.6	0.0 ± 0.0	0.004	-∞
CILP2	IPI00216780	127	0.6 ± 0.2	0.0 ± 0.0	0.007	-∞
COCH	IPI00012386	59	0.6 ± 0.1	0.0 ± 0.0	0.001	-∞
COL18A1	IPI00022822	154	1.8 ± 0.4	0.0 ± 0.0	0.002	-∞
COL6A2	IPI00304840	109	0.9 ± 0.3	0.0 ± 0.0	0.006	-∞
CPE	IPI00031121	64	1.9 ± 0.6	0.0 ± 0.0	0.007	-∞
CXCL16	IPI00004946	30	0.8 ± 0.5	0.0 ± 0.0	0.046	-∞
DKK1	IPI00016353	29	0.8 ± 0.4	0.0 ± 0.0	0.023	-∞
ECM1	IPI00003351	61	0.4 ± 0.1	0.0 ± 0.0	0.001	-∞
F2	IPI00019568	70	0.4 ± 0.1	0.0 ± 0.0	0.001	-∞
FBLN1	IPI00296534	77	0.7 ± 0.2	0.0 ± 0.0	0.007	-∞
FBLN1	IPI00296537	74	1.0 ± 0.1	0.0 ± 0.0	0.000	-∞
FGF19	IPI00032908	24	1.4 ± 0.1	0.0 ± 0.0	0.000	-∞
FN1	IPI00022418	263	1.2 ± 0.5	0.0 ± 0.0	0.013	-∞
FSTL1	IPI00029723	35	1.6 ± 0.9	0.0 ± 0.0	0.046	-∞
FUCA2	IPI00012440	54	0.8 ± 0.0	0.0 ± 0.0	N/A[b]	-∞
GALNT2	IPI00004669	65	1.2 ± 0.6	0.0 ± 0.0	0.017	-∞
GDF15	IPI00306543	34	1.1 ± 0.1	0.0 ± 0.0	0.000	-∞
HAPLN3	IPI00045527	48	1.4 ± 0.4	0.0 ± 0.0	0.003	-∞
HSPG2	IPI00024284	469	7.4 ± 0.9	0.0 ± 0.0	0.000	-∞
IGFBP6	IPI00029235	25	1.5 ± 0.5	0.0 ± 0.0	0.006	-∞
KITLG	IPI00220142	28	1.0 ± 0.1	0.0 ± 0.0	0.000	-∞
KLK10	IPI00480121	30	1.0 ± 0.6	0.0 ± 0.0	0.048	-∞
LAMA3	IPI00377045	367	1.2 ± 0.7	0.0 ± 0.0	0.045	-∞
LAMA5	IPI00783665	400	5.3 ± 1.1	0.0 ± 0.0	0.001	-∞
LAMB1	IPI00013976	198	3.2 ± 0.3	0.0 ± 0.0	0.000	-∞
LAMB2	IPI00296922	196	0.7 ± 0.1	0.0 ± 0.0	0.000	-∞
LAMB3	IPI00299404	130	1.0 ± 0.5	0.0 ± 0.0	0.021	-∞
LAMC1	IPI00298281	178	2.8 ± 0.6	0.0 ± 0.0	0.002	-∞
LAMC2	IPI00015117	131	0.7 ± 0.4	0.0 ± 0.0	0.035	-∞
LCN2	IPI00299547	23	1.8 ± 0.4	0.0 ± 0.0	0.002	-∞
LOXL2	IPI00294839	87	1.0 ± 0.3	0.0 ± 0.0	0.005	-∞
MAMDC2	IPI00183750	78	1.1 ± 0.1	0.0 ± 0.0	0.000	-∞
PAM	IPI00177543	108	2.8 ± 1.2	0.0 ± 0.0	0.013	-∞
PLAT	IPI00019590	63	0.6 ± 0.2	0.0 ± 0.0	0.004	-∞

PLAU	IPI00296180	49	1.0 ± 0.4	0.0 ± 0.0	0.008	-∞
PROS1	IPI00294004	75	0.6 ± 0.3	0.0 ± 0.0	0.021	-∞
QSOX1	IPI00003590	83	7.4 ± 0.3	0.0 ± 0.0	0.000	-∞
RNASE4	IPI00029699	17	1.3 ± 0.3	0.0 ± 0.0	0.001	-∞
SCG2	IPI00009362	71	0.4 ± 0.0	0.0 ± 0.0	N/A	-∞
SERPINE1	IPI00007118	45	1.4 ± 0.6	0.0 ± 0.0	0.017	-∞
SERPINE2	IPI00914848	44	4.5 ± 0.9	0.0 ± 0.0	0.001	-∞
SERPING1	IPI00879931	59	0.5 ± 0.1	0.0 ± 0.0	0.000	-∞
SERPINI1	IPI00016150	46	0.7 ± 0.3	0.0 ± 0.0	0.017	-∞
SPINT1	IPI00376403	58	0.9 ± 0.1	0.0 ± 0.0	0.000	-∞
TF	IPI00945626	63	0.8 ± 0.1	0.0 ± 0.0	0.000	-∞
TGFB1	IPI00000075	44	1.1 ± 0.5	0.0 ± 0.0	0.018	-∞
THBS1	IPI00296099	129	1.1 ± 0.3	0.0 ± 0.0	0.003	-∞
TINAGL1	IPI00005563	52	0.5 ± 0.2	0.0 ± 0.0	0.018	-∞
VCAN	IPI00009802	373	1.4 ± 0.8	0.0 ± 0.0	0.029	-∞
VWA1	IPI00396383	47	0.4 ± 0.2	0.0 ± 0.0	0.019	-∞
COL6A1	IPI00291136	109	7.2 ± 1.7	0.3 ± 0.6	0.002	-4.430
COL12A1	IPI00329573	333	20.9 ± 4.0	1.0 ± 1.0	0.001	-4.382
APP	IPI00219187	83	6.0 ± 0.8	0.3 ± 0.6	0.000	-4.174
PCSK9	IPI00387168	74	6.0 ± 0.4	0.7 ± 0.6	0.000	-3.164
GAS6	IPI00032532	75	2.9 ± 0.1	0.3 ± 0.6	0.002	-3.116
LSR	IPI00409640	71	2.3 ± 0.2	0.3 ± 0.6	0.005	-2.814
TIMP2	IPI00027166	24	2.2 ± 0.5	0.3 ± 0.6	0.015	-2.714
IGFBP2	IPI00297284	35	3.8 ± 0.5	0.7 ± 0.6	0.002	-2.507
MSLN	IPI00793649	71	1.7 ± 0.4	0.3 ± 0.6	0.026	-2.333
KLK6	IPI00023845	27	3.1 ± 0.2	0.7 ± 1.2	0.023	-2.229
FRAS1	IPI00455316	444	3.1 ± 0.4	0.7 ± 1.2	0.027	-2.211
CLU	IPI00400826	58	4.4 ± 0.5	1.0 ± 1.0	0.006	-2.142
NUCB1	IPI00295542	54	2.3 ± 0.5	0.7 ± 0.6	0.021	-1.814
CST6	IPI00019954	17	2.2 ± 0.3	0.7 ± 0.6	0.015	-1.740
CPA4	IPI00008894	47	4.3 ± 1.2	1.3 ± 0.6	0.020	-1.675

[a]Rsc: the $\log_2$ ratio of protein abundance between the GKB-treated and control-treated group calculated using equation (1).
[b]N/A: not available, where standard deviations for both groups were 0.

Table S2. List of the up-regulated secretory proteins (56 proteins).

Gene symbol	Accession #	MW	Mean ± SD of Control	Mean ± SD of GKB treated	*p* value	Rsc[a]
STXBP2	IPI00943192	66	0.1 ± 0.2	9.3 ± 2.9	0.005	6.316
LAMB4	IPI00295437	194	0.1 ± 0.1	5.3 ± 1.5	0.004	6.093
HSPD1	IPI00784154	61	1.4 ± 0.6	75.0 ± 15.7	0.001	5.778
HDLBP	IPI00894287	138	0.1 ± 0.1	4.3 ± 2.1	0.025	5.209
TLN1	IPI00298994	270	1.7 ± 0.6	44.3 ± 6.1	0.000	4.689
CAPZA2	IPI00026182	33	0.5 ± 0.2	10.7 ± 2.1	0.001	4.508
YARS	IPI00007074	59	1.2 ± 0.5	25.0 ± 5.3	0.001	4.368
COPA	IPI00646493	139	0.9 ± 0.4	18.0 ± 7.2	0.015	4.325
AIMP1	IPI00793201	37	0.5 ± 0.3	10.0 ± 3.6	0.011	4.193
RBMX	IPI00304692	42	0.6 ± 0.2	10.3 ± 4.5	0.020	4.047
KARS	IPI00307092	71	0.9 ± 0.4	14.0 ± 2.0	0.000	4.026
CAPZA1	IPI00005969	33	0.9 ± 0.5	14.3 ± 1.2	0.000	3.935
ISG15	IPI00375631	18	0.3 ± 0.2	4.7 ± 1.5	0.008	3.901
PPIA	IPI00419585	18	3.9 ± 0.5	57.7 ± 1.2	0.000	3.870
HMGB1	IPI00419258	25	2.4 ± 0.1	34.7 ± 2.3	0.000	3.839
FLNA	IPI00333541	281	7.6 ± 0.8	105.3 ± 6.0	0.000	3.790
HSPH1	IPI00218993	92	2.3 ± 1.0	31.0 ± 5.6	0.001	3.774
SERPINB5	IPI00783625	42	1.0 ± 0.4	13.3 ± 2.9	0.002	3.715
GARS	IPI00783097	83	3.7 ± 0.8	48.3 ± 9.8	0.001	3.703
ACTN4	IPI00013808	105	9.7 ± 1.1	125.0 ± 11.3	0.000	3.684
C19orf10	IPI00056357	19	0.9 ± 0.1	11.3 ± 1.5	0.000	3.657
ACTN1	IPI00013508	103	6.4 ± 0.9	79.7 ± 14.0	0.001	3.645
PEBP1	IPI00219446	21	2.5 ± 1.0	28.7 ± 6.5	0.002	3.520
TUBA4A	IPI00007750	50	6.3 ± 1.1	70.7 ± 2.3	0.000	3.490
VCL	IPI00307162	124	6.1 ± 1.5	68.3 ± 1.5	0.000	3.478
HMGB2	IPI00219097	24	1.7 ± 0.4	18.3 ± 4.0	0.002	3.415
HDGF	IPI00020956	27	0.6 ± 0.3	6.0 ± 3.0	0.037	3.263
IL18	IPI00290198	22	1.2 ± 0.2	11.3 ± 2.1	0.001	3.227
RNPEP	IPI00642211	73	1.4 ± 0.5	13.3 ± 3.1	0.003	3.206
GPI	IPI00908881	60	6.2 ± 1.2	56.3 ± 4.2	0.000	3.181
TXN	IPI00216298	12	0.9 ± 0.2	8.0 ± 1.7	0.002	3.155
WDR1	IPI00746165	66	3.8 ± 0.3	33.0 ± 2.0	0.000	3.123
TPT1	IPI00550900	20	3.4 ± 0.2	29.7 ± 5.0	0.001	3.110
SORD	IPI00216057	38	2.1 ± 0.8	17.0 ± 2.6	0.001	2.984
P4HB	IPI00010796	57	3.8 ± 0.9	30.0 ± 4.4	0.001	2.970
PRDX4	IPI00011937	31	1.8 ± 0.3	13.3 ± 2.5	0.001	2.923
YBX1	IPI00031812	36	2.4 ± 0.6	18.3 ± 4.9	0.005	2.920
SOD1	IPI00218733	16	2.4 ± 0.3	18.0 ± 2.0	0.000	2.917
CALM3	IPI00075248	17	0.9 ± 0.1	7.0 ± 1.7	0.004	2.901

LGALS1	IPI00219219	15	2.2 ± 1.1	16.3 ± 1.5	0.000	2.901
SFN	IPI00013890	28	5.5 ± 0.6	41.0 ± 2.6	0.000	2.886
ALDOA	IPI00465439	39	17.4 ± 3.4	128.3 ± 8.5	0.000	2.881
SERPINB1	IPI00027444	43	1.9 ± 0.4	13.7 ± 3.8	0.006	2.866
GSR	IPI00759575	52	2.5 ± 0.3	18.0 ± 2.6	0.001	2.848
LGALS3	IPI00465431	26	0.9 ± 0.2	6.7 ± 0.6	0.000	2.830
ANXA2	IPI00418169	40	4.8 ± 0.9	33.0 ± 4.0	0.000	2.768
MIF	IPI00293276	12	0.9 ± 0.6	6.0 ± 2.6	0.032	2.740
CA2	IPI00218414	29	0.9 ± 0.5	5.0 ± 1.0	0.003	2.477
IDE	IPI00220373	118	1.7 ± 0.4	9.3 ± 3.2	0.015	2.441
ALCAM	IPI00015102	65	2.5 ± 0.2	12.3 ± 5.0	0.028	2.280
CALR	IPI00020599	48	2.1 ± 0.2	8.7 ± 2.5	0.011	2.012
HIST1H4B	IPI00453473	11	2.9 ± 0.3	11.7 ± 4.2	0.022	1.994
PSAP	IPI00012503	58	1.5 ± 0.6	5.7 ± 0.6	0.001	1.933
GSN	IPI00026314	86	4.2 ± 0.4	12.0 ± 1.7	0.002	1.522
CD9	IPI00215997	25	2.5 ± 0.4	5.7 ± 1.2	0.012	1.158
GPC4	IPI00232571	62	0.5 ± 0.1	1.0 ± 0.0	0.001	1.093

[a]Rsc: the $\log_2$ ratio of protein abundance between the GKB-treated and the control-treated group calculated using equation (1).

Table S3. Summary of the secretory proteins that have a high degree of interaction.

Gene Symbol	N of interactions[a]	Rsc	GO term related to apoptosis	Function[b]	Ref.
FN1	37	-∞		pro-apoptotic	1
TGFB1	24	-∞	Induction of apoptosis	Induces B lymphoid cell apoptosis by first blocking cells at the G1/S transition, followed by apoptosis	2
APP	22	-∞	Neuron apoptosis	NMDA (N-methyl-D-aspartate) induced neuronal apoptosis was associated with an increase in cytoplasmic APP immunoreactivity	3
HSPD1	16	5.85	Caspase activation, negative or positive regulation of apoptosis	Pro- and anti-apoptotic function	4
SERPINE1	15	-∞	Negative regulation of apoptosis	Anti-apoptotic	5
PLAT	15	-∞		Pro-apoptotic	6
TF	14	-∞		Tumor associated transplantation antigen that can serve as an anti-apoptotic agent	7
PLAU	12	-∞		Anti-apoptotic effect especially in mouse embryonic fibroblasts	8
HSPG2	11	-∞		N.R.[c]	
SERPING1	11	-∞		N.R.	
CLU	11	-1.73	Induction of apoptosis by intracellular signals	Reduction of CLU-induced apoptosis	9
SOD1	11	2.92	DNA fragmentation during apoptosis	Anti-apoptotic	10
TXN	11	3.17		Both anti-apoptotic and anti-inflammatory agent	11
ACTN4	11	3.69	Regulation of apoptosis	Increases the rate of apoptosis by interacting with and activating DNase Y during apoptosis	12

[a]Number of interactions acquired from the STRING analysis.
[b]Apoptosis-related functions described in the references.
[c]No references found in PubMed when the gene name was searched with 'apoptosis'.

Table S4. Summary of the secretory proteins with low degrees of interaction.

Gene symbol	N of interactions[a]	Rsc	GO term related to apoptosis	Function[b]	Ref.
FGF19	0	-∞		Increases proliferation and invasion capabilities of human hepatocellular carcinoma cell lines and inhibits apoptosis	13
FUCA2	0	-∞		N.R.[c]	
KLK10	0	-∞		Changes in KLK expression are not related to apoptosis or cell death	14
MAMDC2	0	-∞		N.R.	
RNASE4	0	-∞		N.R.	
TINAGL1	0	-∞		N.R.	
PCSK9	0	-3.164	positive regulation of neuron apoptosis	Regulates neuronal apoptosis by adjusting ApoER2 levels and signaling	15
LSR	0	-2.814		Not significant	
MSLN	0	-2.333		Inhibits paclitaxel-induced apoptosis through the PI3K pathway	16
FRAS1	0	-2.211		N.R.	
NUCB1	0	-1.814		Induces autoimmune phenomena and thymic apoptosis when exogenously administered to mice	17
CST6	0	-1.740		Anti-apoptotic effect in TNF-α induced apoptosis	18
CPA4	0	-1.675		N.R.	
PSAP	0	1.933		Induces Apaf-1 and Smac-dependent mitochondrial apoptotic pathway	19
HIST1H4B	0	1.994		N.R.	
ALCAM	0	2.280		Induces apoptosis	20
TPT1	0	3.110	anti-apoptosis	Target of p53, thus acts as an anti-apoptotic protein	21
RNPEP	0	3.206		N.R.	
COPA	0	4.325		Knockdown of COPA induces apoptosis and suppresses tumor growth in a mesothelioma mouse model	22
HDLBP	0	5.209		N.R.	
LAMB4	0	6.093		N.R.	
STXBP2	0	6.316		N.R.	

[a]Number of interactions acquired from the STRING analysis.
[b]Apoptosis-related functions described in the references.
[c]No references found in PubMed when the gene name was searched with 'apoptosis'.

Figure S1.

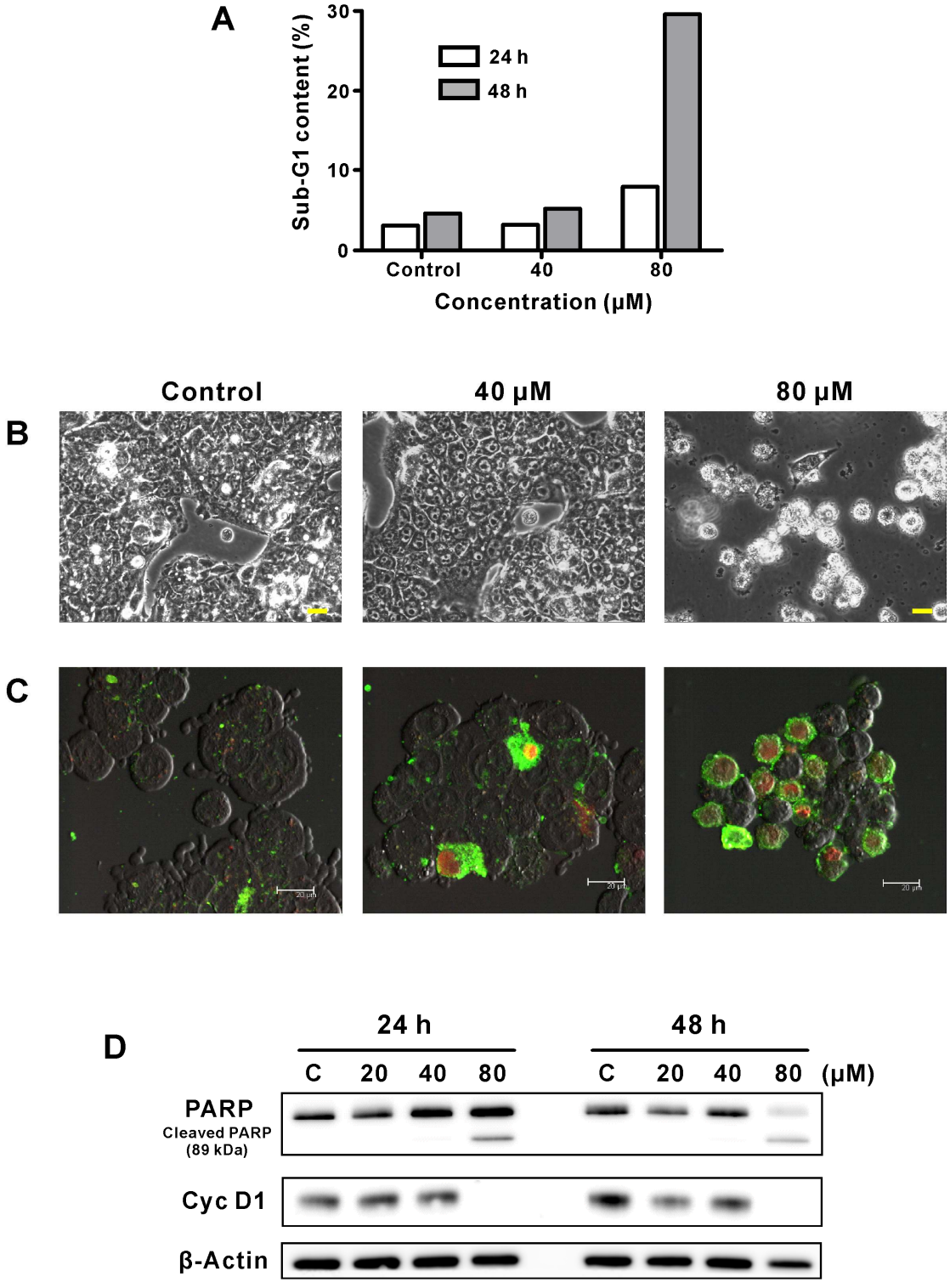

Figure S1. Induction of apoptotic cell death by GKB in HepG2 human hepatoma cells. (A) The sub-G1 content (%) was evaluated by flow cytometric DNA content analysis. HepG2 cells were treated with GKB (40 or 80 μM) for 24 and 48 h. (B, C) Changes in cell morphology. HepG2 cells were treated with GKB (40 or 80 μM) for 48 h. (B) Phase contrast microscope images (bar = 20 μm). (C) Confocal microscope images. The cells were stained with annexin V-fluorescein and propidium iodide (bar = 20 μm). (D) Expression levels of PARP and Cyclin D1 were measured by western blot analysis. HepG2 cells were treated with GKB (20, 40, or 80 μM) for 24 and 48 h.

Figure S2.

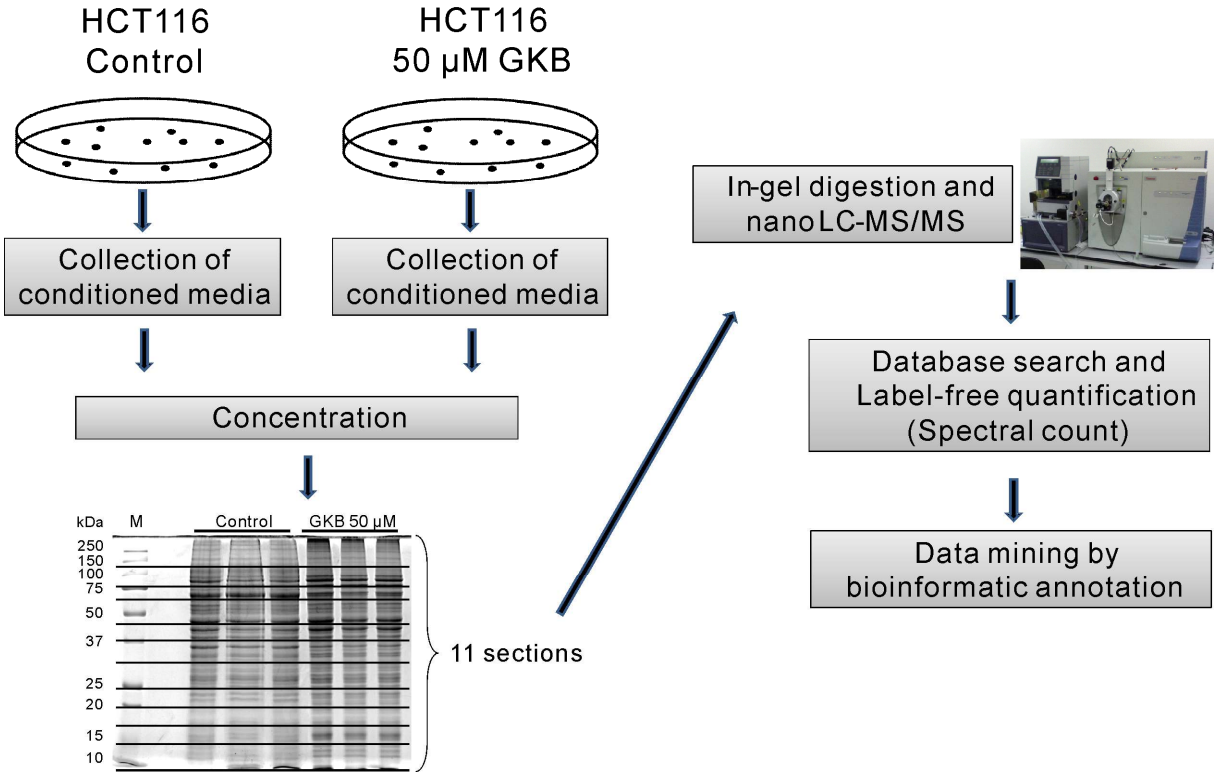

Figure S2. Experimental scheme for the analysis of the secreted proteome of HCT116 cells treated with GKB.

Supporting Information References

1. Sugahara, H.; Kanakura, Y.; Furitsu, T.; Ishihara, K.; Oritani, K.; Ikeda, H.; Kitayama, H.; Ishikawa, J.; Hashimoto, K.; Kanayama, Y., Induction of programmed cell death in human hematopoietic cell lines by fibronectin via its interaction with very late antigen 5. *J. Exp. Med.* **1994**, *179*, 1757-1766.

2. Arsura, M.; Wu, M.; Sonenshein, G. E., TGFβ1 inhibits NF-κB/Rel activity inducing apoptosis of B cells: transcriptional activation of IκBα. *Immunity* **1996**, *5*, 31-40.

3. Lesort, M.; Esclaire, F.; Yardin, C.; Hugon, J., NMDA induces apoptosis and necrosis in neuronal cultures. Increased APP immunoreactivity is linked to apoptotic cells. *Neurosci. Lett.* **1997**, *221*, 213-216.

4. Kim, S.-C.; Stice, J. P.; Chen, L.; Jung, J. S.; Gupta, S.; Wang, Y.; Baumgarten, G.; Trial, J.; Knowlton, A. A., Extracellular heat shock protein 60, cardiac myocytes, and apoptosis. *Circ. Res.* **2009**, *105*, 1186-1195.

5. Chen, Y.; Kelm, R. J.; Budd, R. C.; Sobel, B. E.; Schneider, D. J., Inhibition of apoptosis and caspase-3 in vascular smooth muscle cells by plasminogen activator inhibitor type-1. *J. Cell. Biochem.* **2004**, *92*, 178-188.

6. Kenagy, R. D.; Min, S.-K.; Mulvihill, E.; Clowes, A. W., A link between smooth muscle cell death and extracellular matrix degradation during vascular atrophy. *J. Vasc. Surg.* **2011**, *54*, 182-191.

7. Lesnikov, V.; Lesnikovaa, M.; Deega, H. J., Pro-apoptotic and anti-apoptotic effects of transferrin and transferrin-derived glycans on hematopoietic cells and lymphocytes. *Exp. Hematol.* **2001**, *29*, 477-489.

8. Mazzieri, R.; Furlan, F.; D'Alessio, S.; Zonari, E.; Talotta, F.; Verde, P.; Blasi, F., A direct link between expression of urokinase plasminogen activator receptor, growth rate and oncogenic transformation in mouse embryonic fibroblasts. *Oncogene* **2006**, *26*, 725-732.

9. Yan, Y.; Luo, K.; Zhang, H.; Chai, W., RNA interference-mediated secretory clusterin gene silencing inhibits proliferation and promotes apoptosis of human non-small cell lung cancer cells. *Hepato-Gastroenterology* **2013**, *60*, 70-5.

10. Liang, H.; Arsenault, J.; Mortensen, J.; Park, F.; Johnson, C.; Nilakantan, V., Partial attenuation of cytotoxicity and apoptosis by SOD1 in ischemic renal epithelial cells. *Apoptosis* **2009**, *14*, 1176-1189.

11. Ono, R.; Masaki, T.; Dien, S.; Yu, X.; Fukunaga, A.; Yodoi, J.; Nishigori, C., Suppressive effect of recombinant human thioredoxin on ultraviolet light-induced inflammation and apoptosis in murine skin. *J. Dermatol.* **2012**, *39*, 843-851.

12. Liu, Q. Y.; Lei, J. X.; LeBlanc, J.; Sodja, C.; Ly, D.; Charlebois, C.; Walker, P. R.; Yamada, T.; Hirohashi, S.; Sikorska, M., Regulation of DNaseY activity by actinin-alpha4 during apoptosis. *Cell Death Differ.* **2004**, *11*, 645-654.

13. Miura, S.; Mitsuhashi, N.; Shimizu, H.; Kimura, F.; Yoshidome, H.; Otsuka, M.; Kato, A.; Shida, T.; Okamura, D.; Miyazaki, M., Fibroblast growth factor 19 expression correlates with tumor progression and poorer prognosis of hepatocellular carcinoma. *BMC Cancer* **2012**, *12*, 56.

14. Paliouras, M.; Diamandis, E. P., Intracellular signaling pathways regulate hormone-dependent kallikrein gene expression. *Tumour Biol.* **2008**, *29*, 63-75.

15. Kysenius, K.; Muggalla, P.; Mätlik, K.; Arumäe, U.; Huttunen, H., PCSK9 regulates neuronal apoptosis by adjusting ApoER2 levels and signaling. *Cell. Mol. Life Sci.* **2012**, *69*, 1903-1916.

16. Chang, M. C.; Chen, C. A.; Hsieh, C. Y.; Lee, C. N.; Su, Y. N.; Hu, Y. H.; Cheng, W. F., Mesothelin inhibits paclitaxel-induced apoptosis through the PI3K pathway. *Biochem. J.* **2009**, *424*, 449-448.

17. Kanai, Y.; Kyuwa, S.; Miura, K.; Kurosawa, Y., Induction and natural occurrence of serum nucleosomal DNA in autoimmune MRL/lpr/lpr mice: its relation to apoptosis in the thymus. *Immunol. Lett.* **1995**, *46*, 207-14.

18. Vigneswaran, N.; Wu, J.; Zacharias, W., Upregulation of cystatin M during the progression of oropharyngeal squamous cell carcinoma from primary tumor to metastasis. *Oral Oncol.* **2003**, *39*, 559-568.

19. Li, T.; Zeng, L.; Gao, W.; Cui, M.-Z.; Fu, X.; Xu, X., PSAP induces a unique Apaf-1 and Smac-dependent mitochondrial apoptotic pathway independent of Bcl-2 family proteins. *Biochim. Biophys. Acta* **2013**, *1832*, 453-474.

20. Hein, S.; Müller, V.; Köhler, N.; Wikman, H.; Krenkel, S.; Streichert, T.; Schweizer, M.; Riethdorf, S.; Assmann, V.; Ihnen, M.; Beck, K.; Issa, R.; Jänicke, F.; Pantel, K.; Milde-Langosch, K., Biologic role of activated leukocyte cell adhesion molecule overexpression in breast cancer cell lines and clinical tumor tissue. *Breast Cancer Res. Treat.* **2011**, *129*, 347-360.

21. Chen, W.; Wang, H.; Tao, S.; Zheng, Y.; Wu, W.; Lian, F.; Jaramillo, M.; Fang, D.; Zhang, D. D., Tumor protein translationally controlled 1 is a p53 target gene that promotes cell survival. *Cell Cycle* **2013**, *12*, 2321-2328.

22. Sudo, H.; Tsuji, A. B.; Sugyo, A.; Kohda, M.; Sogawa, C.; Yoshida, C.; Harada, Y.-n.; Hino, O.; Saga, T., Knockdown of COPA, identified by loss-of-function screen, induces apoptosis and suppresses tumor growth in mesothelioma mouse model. *Genomics* **2010**, *95*, 210-216.